WILEY-VCH

DOI: 10.1002/ ((please add manuscript number))
Article type: Full Paper

Single-Component White-Light Emission in Two-Dimensional Hybrid Perovskites with Hybridized Halogen Atoms

Guojun Zhou, Mingze Li, Jing Zhao, Maxim Molokeev, and Zhiguo Xia*

G. J. Zhou, M. Z. Li, Prof. J. Z, Prof. Z. G. Xia
The Beijing Municipal Key Laboratory of New Energy Materials and Technologies,
School of Materials Sciences and Engineering, University of Science and Technology Beijing,
Beijing 100083, P. R. China
E-mail: xiazg@ustb.edu.cn

Prof. Z. G. Xia
State Key Laboratory of Luminescent Materials and Devices and Guangdong Provincial Key Laboratory of Fiber Laser Materials and Applied Techniques,
South China University of Technology, Guangzhou 510641, P.R. China
E-mail: xiazg@scut.edu.cn

Prof. M. S. Molokeev
Laboratory of Crystal Physics
Kirensky Institute of Physics
Federal Research Center KSC SB RAS
Krasnoyarsk 660036, Russia

Prof. M. S. Molokeev
Siberian Federal University
Krasnoyarsk, 660041, Russia

Prof. M. S. Molokeev
Department of Physics
Far Eastern State Transport University
Khabarovsk, 680021, Russia

Keywords: Two-dimensional halide perovskite, Photoluminescence, White-Light Emission

Abstract:

Single-component photoinduced white-light (WL) emission in low-dimensional hybrid halide perovskites has emerged as new generation of luminescence materials; however, the effect of halogens on their intrinsic light emissions and the corresponding mechanisms still left unveiled. Herein, the investigation of a family of two-dimensional (2D) hybrid perovskites $R_2PbBr_{4-x}Cl_x$ (R = BA^+, PMA^+, PEA^+; x = 0, 1, 2, 3, 4) highlights the influence of halogens on the intrinsic emission to reveal the photoluminescence (PL) dependence on the nature and the contribution of the halogens. Ultra-broad emissions covering the entire visible-light region were achieved in the halogen hybrid systems with the stoichiometric of $R_2PbBr_2Cl_2$ (R = BA^+, PMA^+, PEA^+) showing their potential as single-component WL phosphors in solid-state lighting devices. The origin of the WL emissions was due to the synergistic recombination emission of free excitons (FEs) and self-trapped excitons (STEs). The ratio of halogens (Br/Cl) has been verified to be a critical factor to fine-tune the intrinsic emission peroperties. This work provides a feasible strategy to achieve single-component WL emission in 2D hybrid perovskites, and proposes a regulation method of halogen contents for optimizing luminescent properties.

1. Introduction

Hybrid halide perovskites materials have received considerable attention due to their enormous applications in the fields of light-emitting diodes (LEDs),[1] solar cells,[1c, 2] and lasers,[3] etc. Among them, the low-dimensional metal halides are currently becoming a new focus for solid-state lighting because of their good stability and unique broadband emission.[4] Especially, most white-light (WL) emitting perovskite materials reported so far are monolayer two-dimensional (2D) hybrid halides, which opens the exciting prospect of understanding how single-component WL can be generated and also the possibilities of using these materials for solid-state lighting applications.[1a, 4b, 5] In 2014, Karunadasa and coworkers firstly reported two families of 2D layered perovskites (*N*-MEDA)$PbBr_{4-x}Cl_x$ (*N*-MEDA = N^1-methylethane-1, 2-diammonium, x =0-1.2) and (EDBE)PbX_4 (EDBE = 2, 2'-(ethylenedioxy)bis(ethylammonium), X = Cl and Br), which exhibited a stable WL emission and with a relatively high photoluminescence quantum yield (PLQY) of 9% observed in (EDBE)$PbBr_4$.[4b] Since then, several 2D hybrid perovskites, and some one-dimensional (1D) and zero-dimensional (0D) metal halide hybrids have been demonstrated to exhibit WL emission at room temperature.[1b, 5b, 5c, 6] This broadband emission in low-dimensional metal halides is usually associated with structural deformation in the crystal lattice, which induces the self-trapped excitons (STEs) generated from recombination of excited electron-hole pairs through strong electron-phonon coupling.[4e, 6b, 7] Recently, the 2D layered hybrid perovskites, including $(C_6H_5C_2H_4NH_3)_2PbBr_2Cl_2$,[8] $(C_6H_5CH_2NH_3)_2PbBr_{4-x}Cl_x$,[9] and $(CH_3CH_2NH_3)_4Pb_3Br_{10-x}Cl_x$,[6b] were also found to be WL emitters. These results clarified the effect of halogens on STE emissions, and it is generally accepted that it is strongly correlated to the structural distortion of the perovskite layers in the ground state.[7c] However, the precise WL emission mechanism in these materials is still under debate, because only the role of halogens on STEs was investigated, while the effect of halogens on free excitons (FEs) and

the transmissions between FEs and STEs were ignored.[5b, 7b, 10] Thus, it is essential to study the luminescent mechanism to further understand the role of halogens on the intrinsic emissions. In view of this, one can then artificially manipulate the broadband emission of 2D halide perovskites through fine-tuning the type and proportion of halogens.

Herein, we introduce a family of 2D hybrid perovskites $R_2PbBr_{4-x}Cl_x$ (R = BA^+, PMA^+, PEA^+; x = 0, 1, 2, 3, 4) to verify the fundamental relationship between the halogen content and the luminescent properties. The intrinsic light emissions of these compounds showed a strong dependence on the nature and the ratio of the halogens, and a general theory was proposed to explain the broadband emission in 2D hybrid perovskites. Specifically, WL emissions were achieved in the halogen hybrid system $R_2PbBr_2Cl_2$ (R = BA^+, PMA^+, PEA^+) showing their potential as single-component WL phosphors for use with ultraviolet light emitting diodes in solid-state lighting devices. Our realizable cases could provide a new understanding of halogen content on the broadband emission, and propose a feasible strategy to achieve single-component WL emission in 2D hybrid perovskites.

2. Result and discussion

A series of 2D hybrid perovskites were synthesized by a co-precipitation method with different raw material ratios. Rietveld refinements (**Figure S1**, **S2**, and **S3**) indicate that the as-prepared compounds $R_2PbBr_{4-x}Cl_x$ (R = BA^+, PMA^+, PEA^+; x = 0, 1, 2, 3, 4) were of pure phase, and the Br/Cl ratio was taken from the suggested chemical formula and fixed as it is. As shown in **Figure 1a**, regardless of the different organic ligands of BA, PMA or PEA, all of the as-synthesized compounds consist of ⟨100⟩-oriented monolayers formed by coner-sharing $Pb(Br,Cl)_6$ octahedra.[11] The difference in organic cations does not affect the layered structural characteristics because they all form new geometries of hydrogen bonds N-H ... (Br / Cl) corresponding to the rotation of organic cations. Currently one cannot get reliable H-bond parameters because organic molecules were refined as a rigid bulk and the refined C, N,

H atoms present relatively large esd's. Anyway, the 2D layered structure type with corner-sharing $Pb(Br,Cl)_6$ octahedra is reliable. Based on this, main parameters of processing and refinement of $R_2PbBr_{4-x}Cl_x$ (R = BA^+, PMA^+, PEA^+; x = 0, 1, 2, 3, 4) are listed in **Table S1**. The corresponding cell volumes $V(x)$ decrease with Cl(x) concentration increasing (**Figure 1b**), which is in good agreement with the fact that the Cl ion radius (1.81 Å) is smaller than Br ion radius (1.96 Å).[12] The refinements prove that the suggested chemical formulas are close to the real ratio of raw materials.

As shown in **Figure 1c**, the luminescence characteristics of $R_2PbBr_{4-x}Cl_x$ (R = BA^+, PMA^+, PEA^+; x = 0, 1, 2, 3, 4) can be visualized under 365 nm UV lamp, which clearly show the variation trend of emission when Br ions are gradually substituted by Cl ions. Interestingly, all the above-mentioned 2D halogen hybrid perovskites can emit white light, especially in the intermediate composition with x = 2. In order to further evaluate the luminescent properties after halogen ion exchange, diffuse reflectance data were measured (**Figure S4**) and the corresponding band gap values showed an increasing trend with the increase of Cl ions, as shown in **Figure 1d**. The results indicate the relative energy levels before and after halogen ion exchange for these 2D halogen hybrid perovskites, which can be used to analyze the recombination of free excitons (FEs).

Figure 2a, b, c display the normalized excitation and emission spectra of $BA_2PbBr_{4-x}Cl_x$ (x = 0, 1, 2, 3, 4), $PMA_2PbBr_{4-x}Cl_x$ (x = 0, 1, 2, 3, 4), and $PEA_2PbBr_{4-x}Cl_x$ (x = 0, 1, 2, 3, 4), respectively. As expected, as the Cl concentration (x) increases, all the emission spectra gradually change from a narrow band to ultra-broad dual band consisting of a narrow FES and a broad peak, and eventually mainly show one broad emission band. The narrow band peaks have small Stokes shifts, while the broadband peaks have large Stokes shifts.[1b, 13] Therefore, the narrow band emission is attributed to the recombination of FEs, and the broadband emission is due to the recombination of self-trapped excitons (STEs). In view of this, it can be

concluded that the hybridization of the halogen component not only regulates the free exciton emissions, but also induces the broadband emission from the STEs.

Meanwhile, the overall broadness of the emission is heavily influenced by the structural distortion, which is evaluated here by the level of the distortion of the PbX_6 (X = Br, Cl) octahedra. The distortions of the octahedra were calculated by the following formula: $\Delta d = \left(\frac{1}{6}\right)\sum\left[\frac{d_n - d}{d}\right]^2$, where d is the average bond length and d_n is the individual Pb-Br/Cl bond length.[5b] The distortion indexs of $R_2PbBr_{4-x}Cl_x$ (R = BA^+, PMA^+, x = 0, 1, 2, 3, 4) are shown in **Figure S5**, the compounds with x = 2 showed the relatively high values. since the distortion degree is proportional to the trap depth of STEs, $R_2PbBr_2Cl_2$ pocesses the lowest STE energy.[9-10] In addition, the dependence of full-width at half-maximum (FWHM) values on the halogen contents is shown in **Figure 2d**, and the maximum values of the $R_2PbBr_2Cl_2$ (R = BA^+, PMA^+, PEA^+) systems are 330 nm, 278 nm, and 311nm, respectively. It is obvius that the broadband emission of $R_2PbBr_2Cl_2$ (R = BA^+, PMA^+, PEA^+) originates from the coupling effect of FEs and STEs. To further evaluate the luminencent performance of this series of compounds, the photoluminescence quantum yields (PLQYs) are measured at room temperature, as listed in **Table 1**. The PLQYs of $R_2PbBr_2Cl_2$ (R = BA^+, PMA^+, PEA^+) phosphors are 2.03 %, 4.21%, 6.28 %, respectively. As Br ions are gradually substituted by Cl ions, the values of PLQYs show a tendency to decrease, indicating that the quantum yield of STEs is lower than that of FEs.

As a powerful evidence to certify the luminescent mechanism, the decay curves of $R_2PbBr_2Cl_2$ (R = BA^+, PMA^+, PEA^+) are measured at different monitoring wavelengths. As illustrated in **Figure 3a, b, c**, the PL decay curves monitored at λ_{em} = 380 and 390 nm are fitted by a double exponential decay process with $I = A_1\exp(-t/\tau_1)+A_2\exp(-t/\tau_2)$, and the average lifetimes can be obtained by using the calculation formula $\tau = (A_1\tau_1^2+A_2\tau_2^2)/(A_1\tau_1+A_2\tau_2)$ with the values of 0.72 ns and 2.91 ns for 380 nm and 390 nm

emission, respectively.[14] It is noteworthy that the decay curves of $R_2PbBr_2Cl_2$ (R = BA^+, PMA^+, PEA^+) monitored at the peaks of 542, 520, 540 nm, respectively, tend to become single exponential function ($I = I_0 + A\exp(-t/\tau)$). It is inferred that there is one form of radiation transition with relatively long lifetimes of 5.21, 9.51, and 12.56 ns for $R_2PbBr_2Cl_2$ with R equaling to BA^+, PMA^+, PEA^+, respectively, attributing to the recombination of STEs. As described above, the lifetime at the monitoring wavelength of 380 nm is significantly shorter than that of 390 nm, and thus we believe that the lifetime measured at 380 nm is the real lifetime of FE recombination, while the lifetime at 390 nm is ascribed to the superposition of FEs and STEs. This also indicates that the broadband emissions of $R_2PbBr_2Cl_2$ (R = BA^+, PMA^+, PEA^+) are produced by the coupling of FEs and STEs. In order to further reveal the luminescent mechanism of the hybrid intermediate systems, the dependence of lifetimes of (d) $BA_2PbBr_2Cl_2$, (e) $PMA_2PbBr_2Cl_2$, and (f) $PEA_2PbBr_2Cl_2$ on the emission wavelengths were explored in detail (**Figure 3d, e, f**). The lifetime values at the broadband emission attributed to the STEs are close and continuous, and thus we propose that there are many self-trapped energy levels, which is the fundamental reason for inducing broadband emission of STEs. Based on that, we provide a schematic diagram of the luminescent mechanism of the 2D hybrid perovskites (**Figure 4a, b, c**). In the end member for Br_4 system with a relatively small band gap, the lower energy level position allows the excited electrons to recombine as free excitons, so that one can only observe narrow band emissions originated from Fes process. For the hybrid Br_2Cl_2 system, the levels of FEs and STEs are close to each other, which achieves dual emission due to the balance of energy transfer, resulting in broadband WL emission covering the entire visible-light region. In contrast, in the end member for Cl_4 system, the high level of the free excitons allows most of the energy to be transferred to the STEs, which causes single broadband emissions of STEs as observed. However, in general, the luminescent efficiency of STEs in Cl_4 systems is low, which limits their application as a potential candidate for a single-component white-light emitter. The

above results reveal that the broadband WL emission covering the entire visible-light region could be achieved in the halogen hybrid systems $R_2PbBr_2Cl_2$ (R = BA^+, PMA^+, PEA^+), and thus they are promising as single-component white-light phosphors for use with ultraviolet lightemitting diodes in solid-state lighting devices.

Conclusion

In summary, we have desigened and synthesied a series of hybrid perovskites compounds $R_2PbBr_{4-x}Cl_x$ (R = BA^+, PMA^+, PEA^+; x = 0, 1, 2, 3, 4) with the same 2D ⟨100⟩-oriented layered structures. The nature and the propotion of the halogens were verified to be a key parameter to tune the energy levels of the FEs and STEs. The broadband emissions covering the entire visible-light region were obtained in the halogen hybrid system $R_2PbBr_2Cl_2$ (R = BA^+, PMA^+, PEA^+), which originate from the synergistic effects of the recombination emission of FEs and STEs. Meanwhile, this work demonstrates that fine-tuning the halogen content in 2D hybrid perovskites is a facile way to achieve single-component WL emission. Our case study provide a feasible strategy towords rationally design single-component WL phosphors in hybrid luminescent metal halide which is suitable for solid state lighting.

Experimental Section

Materials and Preparation: $PbCl_2$, $PbBr_2$ (99.9 %, Aladdin), $C_4H_9NH_3Cl$ and $C_4H_9NH_3Br$ (Butylamine hydrochloride (BACl), Butylamine hydrobromide (BABr), 99.9 %, Xi'an p-OLED), $C_6H_5CH_2NH_3Cl$ and $C_6H_5CH_2NH_3Br$ (Benzylamine hydrochloride (PMACl), Benzylamine hydrobromide (PMABr), 99.9 %, Xi'an p-OLED), $C_6H_5CH_2CH_2NH_3Cl$ and $C_6H_5CH_2CH_2NH_3Br$ (2-Phenylethanamine hydrochloride (PEACl), 2-Phenylethanamine hydrobromide (PEABr), 99.9 %, Xi'an p-OLED), C_7H_8 (Toluene 99.5 %, Sinopharm), $C_4H_{10}O$ (Ethyl ether 99.7 %, Sinopharm), DMF (99.5 %, Aladdin). All chemicals were used as received.

The compounds $R_2PbBr_{4-x}Cl_x$ (R = BA^+, PMA^+, PEA^+; x = 0, 1, 2, 3, 4) were synthesized by solution co-precipitation method. The precursors BACl/BABr, PMACl/PMABr, PEACl/PEABr (2 mmol) and $PbCl_2$/ $PbBr_2$ (1 mmol) were dissolved in 2 mL DMF and heated to 90 °C. Toluene was added to the hot clear solution until the solution began to become cloudy. The products $R_2PbBr_{4-x}Cl_x$ (R = BA^+, PMA^+, PEA^+; x = 0, 1, 2, 3, 4) were thus obtained and washed repeatedly with ethyl ether. After filtration, the precursors were dried at 60 °C for 24 h in a vacuum oven. Halogen hybrids were obtained by adjusting the proportions of precursors and lead halide.

Characterization: The powder diffraction data of $R_2PbBr_{4-x}Cl_x$ (R = BA^+, PMA^+, PEA^+; x = 0, 1, 2, 3, 4) for Rietveld analysis were collected at room temperature with an Aeris X-ray diffractometer (Cu-Kα radiation). The step size of 2θ was 0.013°, and the counting time was 5 s per step. The Rietveld refinements were performed by using TOPAS 4.2. The photoluminescence (PL), photoluminescence excitation (PLE) spectra, luminescence decay curves and photoluminescence quantum yields (PLQYs) were measured by FLSP9200 fluorescence spectrophotometer (Edinburgh Instruments Ltd., U. K.). The diffuse reflectance spectra were collected by the Hitachi UH4150 US–vis–near-infrared spectrophotometer using white $BaSO_4$ for calibration.

Supporting Information

Supporting Information is available from the Wiley Online Library or from the author.

Acknowledgements

The present work was supported by the National Natural Science Foundations of China (Grant No. 51722202, 91622125 and 51572023), Natural Science Foundations of Beijing (2172036), Fundamental Research Funds for the Central Universities (FRF-TP-18-002C1 and FRF-TP-18-005A1), and the Guangdong Provincial Science & Technology Project (No. 2018A050506004).

Received: ((will be filled in by the editorial staff))
Revised: ((will be filled in by the editorial staff))
Published online: ((will be filled in by the editorial staff))

References

[1] a) Y. Tian, C. K. Zhou, M. Worku, X. Wang, Y. C. Ling, H. W. Gao, Y. Zhou, Y. Miao, J. j. Guan, B. W. Ma, *Adv. Mater.* **2018**, *30*, 1707093; b) M. D. Smith, B. A. Connor, H. I. Karunadasa, *Chem. Rev.* **2019**, *119*, 3104-3139; c) P. Chen, Y. Bai, M. Q. Lyu, J. H. Yun, M. M. Hao, L. Z. Wang, *Solar. RRL.* **2018**, *2*, 1700186; d) S. Adjokatse, H. H. Fang, M. A. Loi, *Mater. Today.* **2017**, *20*, 413-424.

[2] a) D. H. Cao, C. C. Stoumpos, O. K. Farha, J. T. Hupp, M. G. Kanatzidis, *J. Am. Chem. Soc.* **2015**, *137*, 7843-7850; b) W. Fu, J. Wang, L. Zuo, K. Gao, F. Liu, D. S. Ginger, A. K. Y. Jen, *ACS Energy. Lett.* **2018**, *3*, 2086-2093.

[3] Q. Zhang, R. Su, W. N. Du, X. F. Liu, L. Y. Zhao, S. T. Ha, Q. H. Xiong, *Small. Methods.* **2017**, *1*, 1700163.

[4] a) M. I. Saidaminov, O. F. Mohammed, O. M. Bakr, *ACS Energy. Lett.* **2017**, *2*, 889-896; b) E. R. Dohner, A. Jaffe, L. R. Bradshaw, H. I. Karunadasa, *J. Am. Chem. Soc.* **2014**, *136*, 13154-13157; c) Z. W. Xiao, Z. N. Song, Y. F. Yan, *Adv. Mater.* **2019**, 1803792; d) G. H. Wu, C. K. Zhou, W. M. Ming, D. Han, S. Y. Chen, D. Yang, T. Besara, J. Neu, T. Siegrist, M. H. Du, B. W. Ma, A. Dong, *ACS Energy. Lett.* **2018**, *3*, 1443-1449; e) C. K. Zhou, H. Lin, S. Lee, M. Chaaban, B. W. Ma, *Mater. Res. Lett.* **2018**, *6*, 552-569.

[5] a) E. R. Dohner, E. T. Hoke, H. I. Karunadasa, *J. Am. Chem. Soc.* **2014**, *136*, 1718-1721; b) L. L. Mao, Y. Wu, C. C. Stoumpos, M. R. Wasielewski, M. G. Kanatzidis, *J. Am. Chem. Soc.* **2017**, *139*, 5210-5215; c) H. W. Hu, F. Meier, D. M. Zhao, Y. Abe, Y. Gao, B. B. Chen, T. Salim, E. E. M. Chia, X. F. Qiao, C. Deibel, Y. M. Lam, *Adv. Mater.* **2018**, *30*, 1707621; d) L. T. Dou, A. B. Wong, Y. Yu, M. L. Lai, N. Kornienko, S. W. Eaton, A. Fu, C. G. Bischak, J. Ma, T. Ding, N. S. Ginsberg, L. W. Wang, A. P. Alivisatos, P. D. Yang, *Science.* **2015**, *349*, 1518-1521.

[6] a) Z. Yuan, C. K. Zhou, J. Messier, Y. Tian, Y. Shu, J. M. Wang, Y. Xin, B. W. Ma, *Adv. Opt. Mater.* **2016**, *4*, 2009-2015; b) L. L. Mao, Y. L. Wu, C. C. Stoumpos, B. Traore, C. Katan, J. Even, M. R. Wasielewski, M. G. Kanatzidis, *J. Am. Chem. Soc.* **2017**, *139*, 11956-11963; c) L. L. Mao, P. J. Guo, M. Kepenekian, I. Hadar, C. Katan, J. Even, R. D. Schaller, C. C. Stoumpos, M. G. Kanatzidis, *J. Am. Chem. Soc.* **2018**, *140*, 13078-13088; d) Z. Y. Wu, C. M. Ji, Z. H. Sun, S. S. Wang, S. G. Zhao, W. C. Zhang, L. N. Li, J. H. Luo, *J. Mater. Chem. C.* **2018**, *6*, 1171-1175.

[7] a) X. T. Li, P. J. Guo, M. Kepenekian, I. Hadar, C. Katan, J. Even, C. C. Stoumpos, R. D. Schaller, M. G. Kanatzidis, *Chem. Mater.* **2019**, *31*, 3582-3590; b) T. Hu, M. D. Smith, E. R. Dohner, M. J. Sher, X. Wu, M. T. Trinh, A. Fisher, J. Corbett, X. Y. Zhu, H. I. Karunadasa, A. M. Lindenberg, *J. Phys. Chem. Lett.* **2016**, *7*, 2258-2263; c) M. D. Smith, H. I. Karunadasa, *Acc. Chem. Res.* **2018**, *51*, 619-627.

[8] a) S. Yang, Z. Lin, J. Wang, Y. Chen, Z. Liu, E. Yang, J. Zhang, Q. Ling, *ACS Appl. Mater. Inter.* **2018**, *10*, 15980-15987; b) P. Q. Cai, X. F. Wang, H. J. Seo, X. H. Yan, *Appl. Phys. Lett.* **2018**, *112*, 153901.

[9] M. H. Jung, *Inorg. Chem.* **2019**, *58*, 6748-6757.

[10] M. D. Smith, A. Jaffe, E. R. Dohner, A. M. Lindenberg, H. I. Karunadasa, *Chem. Sci.* **2017**, *8*, 4497-4504.

[11] D. B. Mitzi, S. Wang, C. A. Feild, C. A. Chess, A. M. Guloy, *Science.* **1995**, *267*, 1473-1476.

[12] R. D. Shannon, *Acta Cryst . A* **1976**, *32*, 751-767.

[13] M. D. Smith, B. L. Watson, R. H. Dauskardt, H. I. Karunadasa, *Chem. Mater.* **2017**, *29*, 7083-7087.

[14] C. H. Huang, T. M. Chen, W. R. Liu, Y. C. Chiu, Y. T. Yeh, S. M. Jang, *ACS Appl. Mater. Inter.* **2010**, *2*, 259-264.

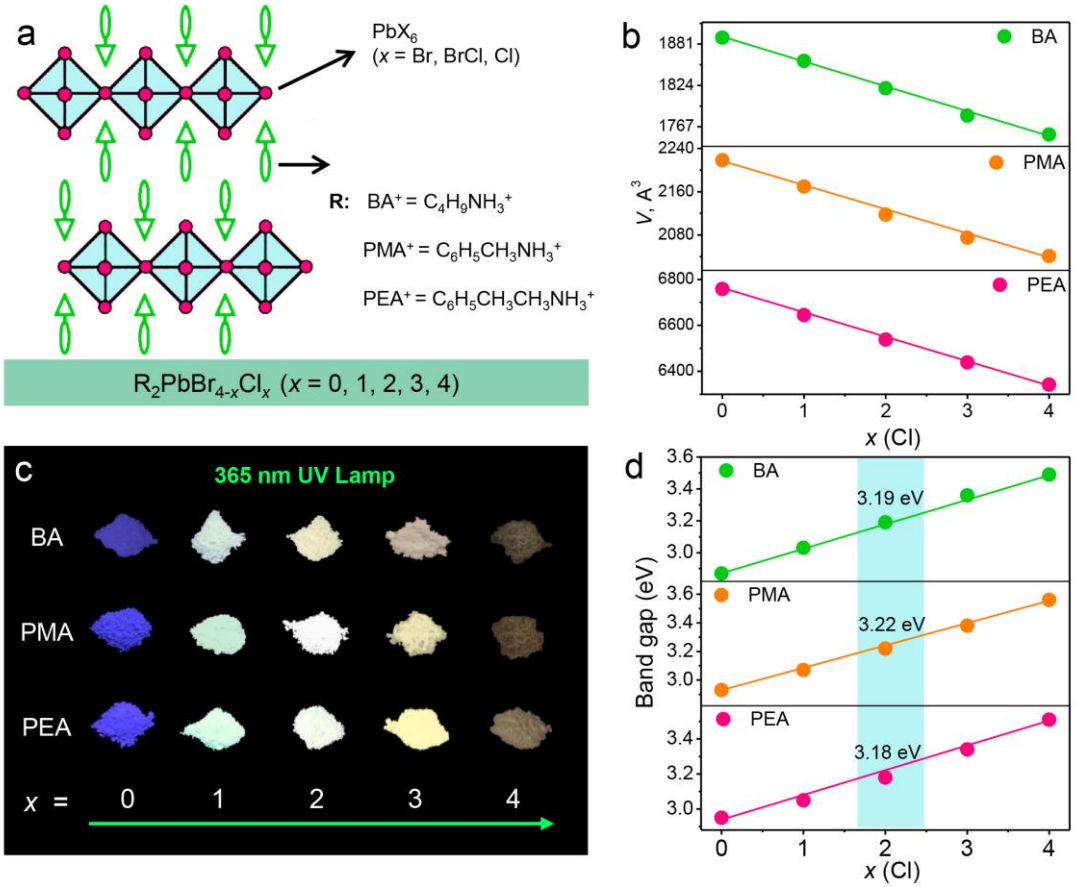

Figure 1. (a) The crystal structure of 2D hybrid perovskites with the general formula $R_2PbBr_{4-x}Cl_x$ (R = BA^+, PMA^+, PEA^+; x = 0, 1, 2, 3, 4). (b) The variable trends of the cell volumes of $R_2PbBr_{4-x}Cl_x$ (R = BA^+, PMA^+, PEA^+) with different halogen concentrations. (c) The luminescent photographs of $R_2PbBr_{4-x}Cl_x$ (R = BA^+, PMA^+, PEA^+; x = 0, 1, 2, 3, 4) phosphors under 365 nm UV lamp. (d) The variable trends of band gaps of $R_2PbBr_{4-x}Cl_x$ (R = BA^+, PMA^+, PEA^+) phosphors with different halogen concentrations.

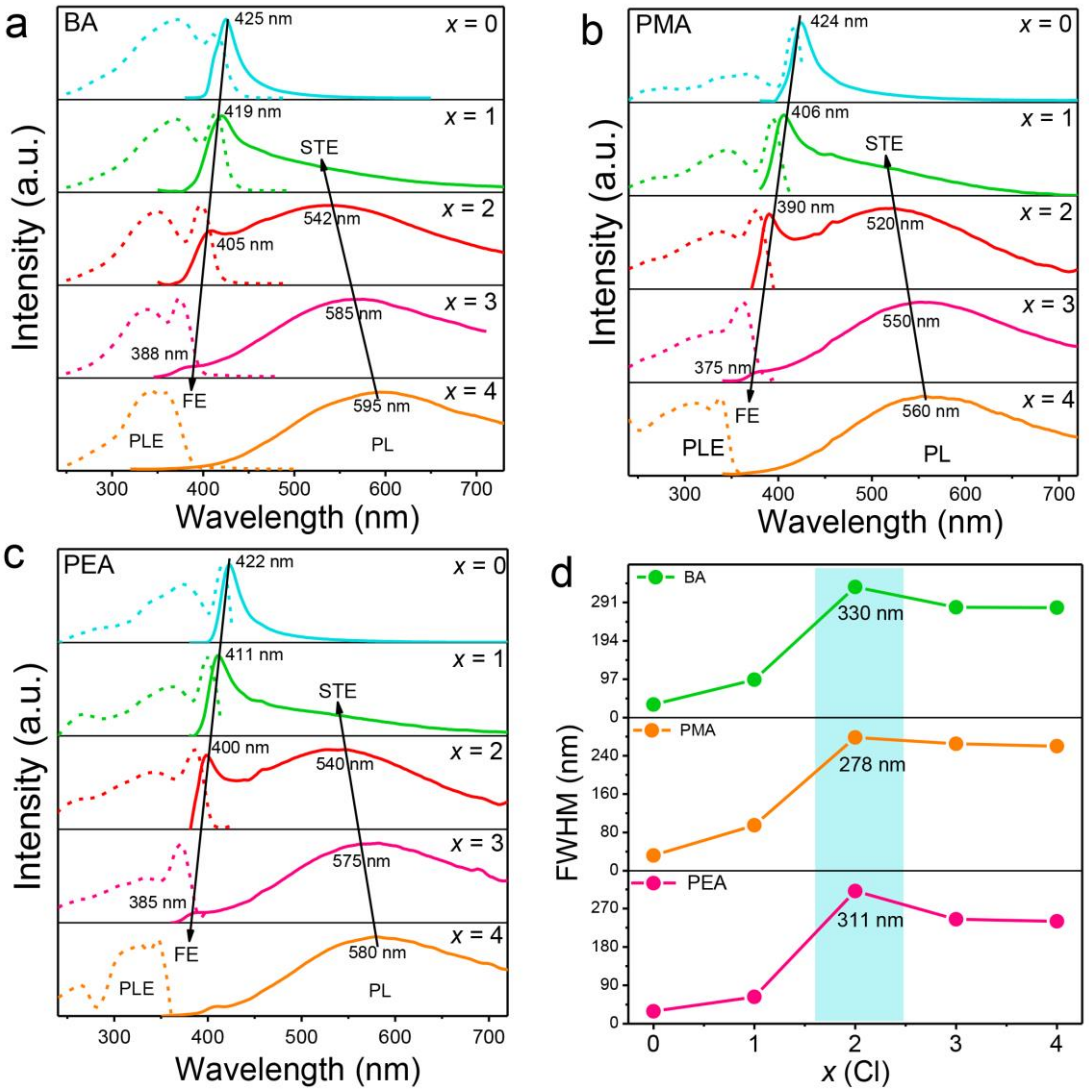

Figure 2. The photoluminescence (PL) and photoluminescence excitation (PLE) spectra of (a) $BA_2PbBr_{4-x}Cl_x$, (b) $PMA_2PbBr_{4-x}Cl_x$, and (c) $PEA_2PbBr_{4-x}Cl_x$ with different halogen ratios; the arrows show variable trends of the narrowband emission of free excitons (FEs) and the broadband emission of self-traped excitons (STEs). (d) The dependence of FWHM values on the halogen contents with the hybrid systems of $R_2PbBr_2Cl_2$ ($R = BA^+$, PMA^+, PEA^+) showing the maximum values of 330, 278 and 311 nm, respectively.

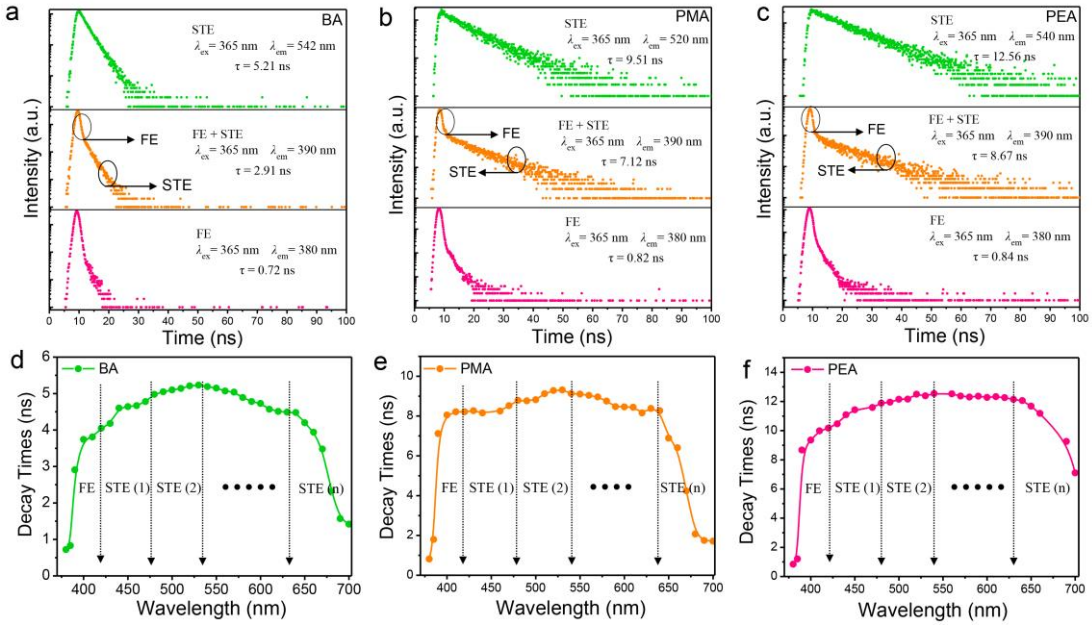

Figure 3. The photoluminescent decay curves of (a) $BA_2PbBr_2Cl_2$, (b) $PMA_2PbBr_2Cl_2$, and (c) $PEA_2PbBr_2Cl_2$ under 365 nm excitation. The dependence of lifetimes of (d) $BA_2PbBr_2Cl_2$, (e) $PMA_2PbBr_2Cl_2$, and (f) $PEA_2PbBr_2Cl_2$ on the variation of monitoring emission wavelengths.

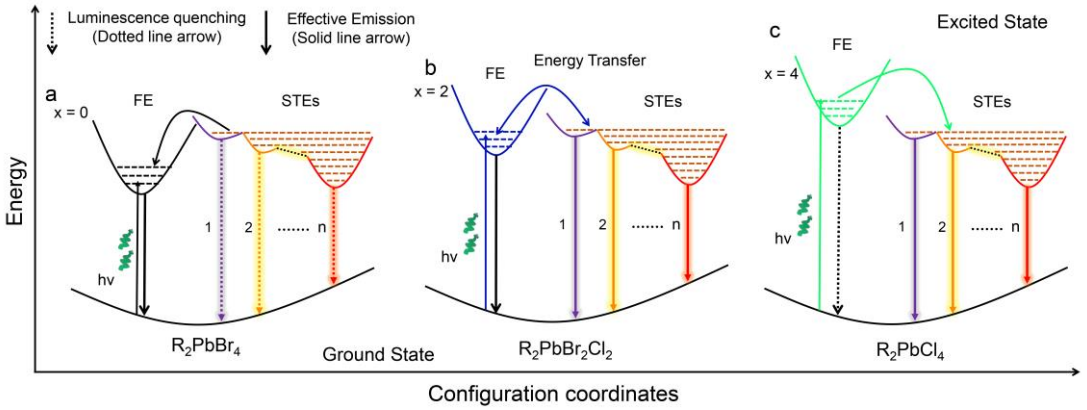

Figure 4. Schematic luminescence mechanism of 2D hybrid perovskites with the recombinations of free excitons and self-traped excitons: (a) R_2PbBr_4; (b) $R_2PbBr_2Cl_2$; (c) R_2PbCl_4.

Table 1. The photoluminescence quantum yields (PLQYs) of $R_2PbBr_{4-x}Cl_x$ (R = BA^+, PMA^+, PEA^+; x = 0, 1, 2, 3, 4).

PLQY (%)	$x = 0$	$x = 1$	$x = 2$	$x = 3$	$x = 4$
BA	9.4	6.43	2.03	0.99	0.63
PMA	7.35	5.25	4.21	0.63	2.39
PEA	12.56	11.68	6.28	2.86	1.56

Table of Contents entry

Single-component photoinduced white-light (WL) emission in low-dimensional hybrid halide perovskites has emerged as new generation of luminescence materials. Herein, the investigation of two-dimensional (2D) hybrid perovskites $R_2PbBr_{4-x}Cl_x$ (R = BA^+, PMA^+, PEA^+; x = 0, 1, 2, 3, 4) highlights the influence of halogens on the intrinsic emission, and the origin of the WL emissions was due to the synergistic recombination emission of free excitons (FEs) and self-trapped excitons (STEs). This work provides a feasible strategy to achieve single-component WL emission in 2D hybrid perovskites.

Keywords: Two-dimensional halide perovskite, Photoluminescence, White-Light Emission

Guojun Zhou, Mingze Li, Jing Zhao, Maxim Molokeev, and Zhiguo Xia*

Single-Component White-Light Emission in Two-Dimensional Hybrid Perovskites with Hybridized Halogen Atoms

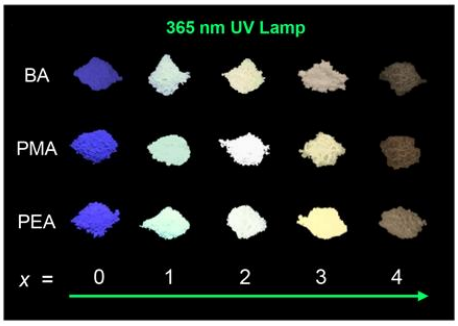

Supporting Information

Single-Component White-Light Emission in Two-Dimensional Hybrid Perovskites with Hybridized Halogen Atoms

*Guojun Zhou, Mingze Li, Jing Zhao, Maxim Molokeev, and Zhiguo Xia**

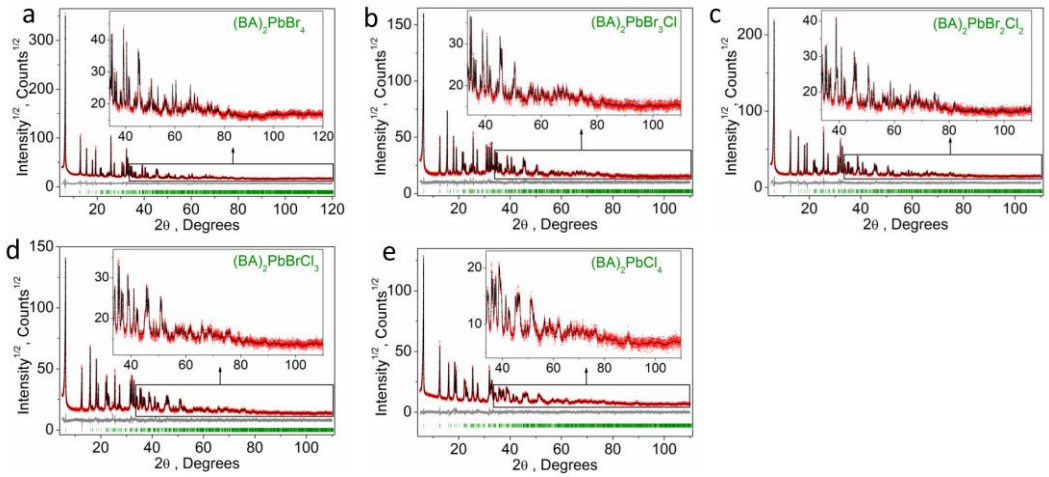

Figure S1. Rietveld refinement patterns of (a) BA_2PbBr_4, (b) BA_2PbBr_3Cl, (c) $BA_2PbBr_2Cl_2$, (d) $BA_2PbBrCl_3$, and (e) BA_2PbCl_4.

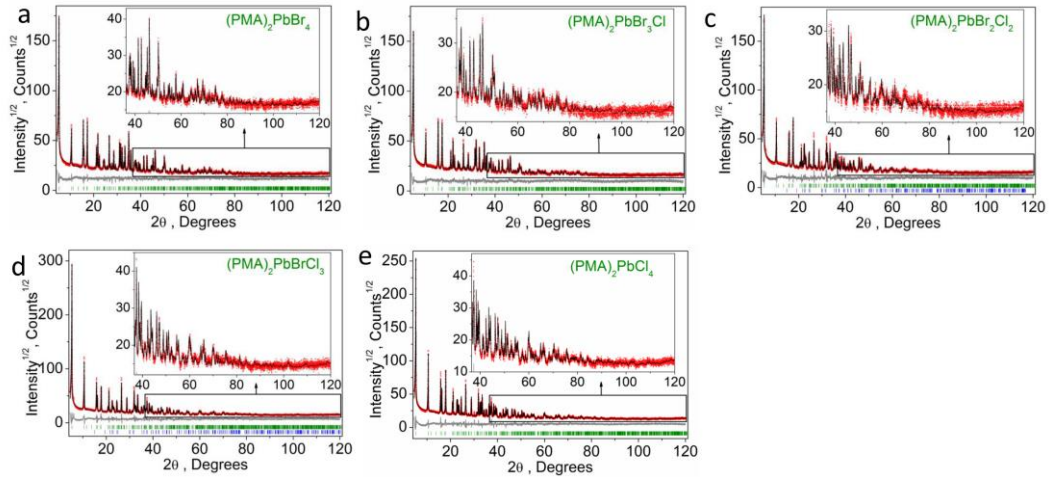

Figure S2. Rietveld refinement patterns of (a) PMA_2PbBr_4, (b) PMA_2PbBr_3Cl, (c) $PMA_2PbBr_2Cl_2$, (d) $PMA_2PbBrCl_3$, and (e) PMA_2PbCl_4.

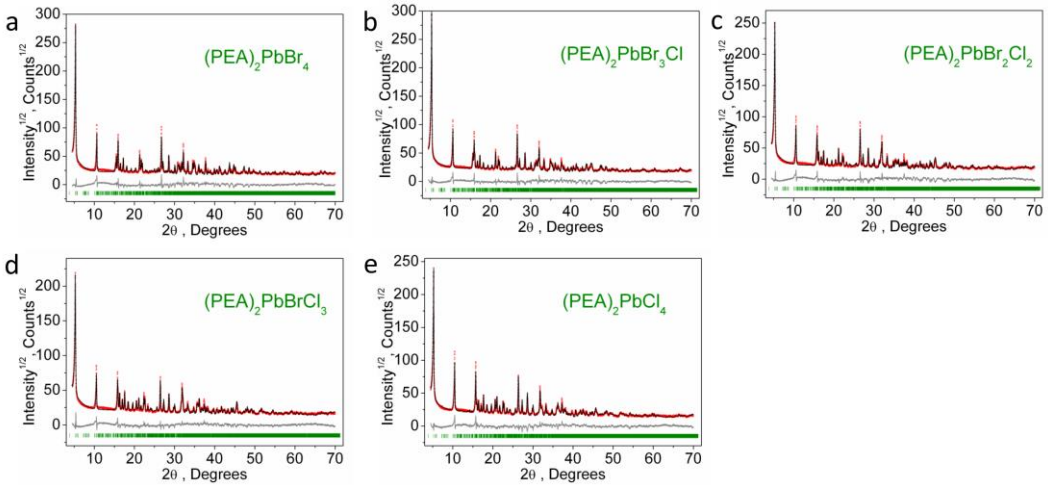

Figure S3. Rietveld refinement patterns of (a) PEA_2PbBr_4, (b) PEA_2PbBr_3Cl, (c) $PEA_2PbBr_2Cl_2$, (d) $PEA_2PbBrCl_3$, and (e) PEA_2PbCl_4.

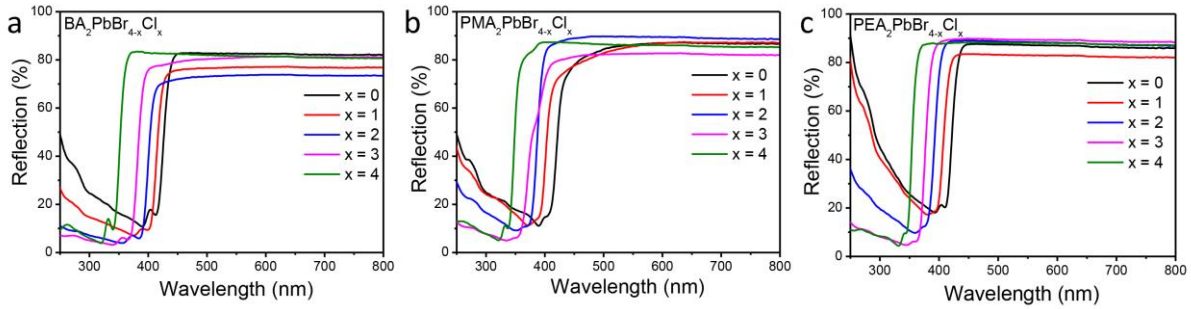

Figure S4. The UV-Vis diffuse reflectance spectra with different halogen contents of $R_2PbBr_{4-x}Cl_x$ (R = BA^+, PMA^+, PEA^+; x = 0, 1, 2, 3, 4).

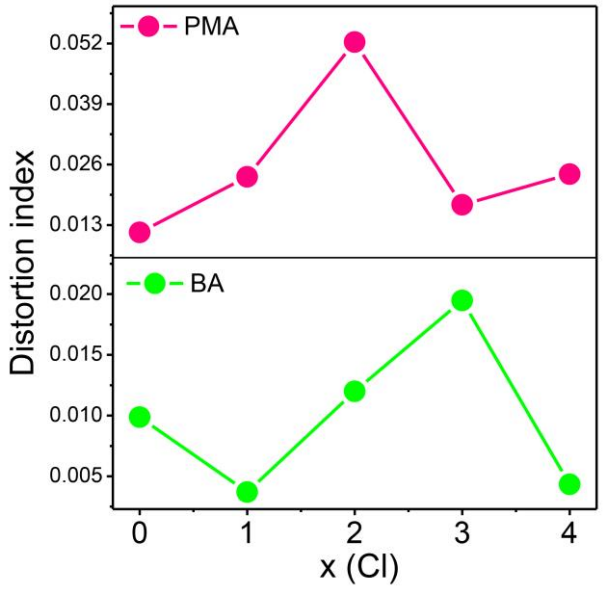

Figure S5. The $Pb(Br,Cl)_6$ octahedra distortion index dependence per x in the compounds $R_2PbBr_{4-x}Cl_x$ (R = BA^+, PMA^+, PEA^+; x = 0, 1, 2, 3, 4).

Table S1. Main parameters of processing and refinement of $R_2PbBr_{4-x}Cl_x$ (R = BA^+, PMA^+, PEA^+; x = 0, 1, 2, 3, 4).

x	Compound	Space group	Cell parameters (º, Å), Cell volume (Å^3)	R_{wp}, R_p (%), χ^2	R_B (%)
0	$(BA)_2PbBr_4$	*Pbca*	*a* = 8.3373 (2), *b* = 8.2177 (2), *c* = 27.5828 (4), *V* = 1889.78 (7)	7.65, 5.90, 1.91	1.49
1	$(BA)_2PbBr_3Cl$	*Pbca*	*a* = 8.2522 (3), *b* = 8.1242 (3), *c* = 27.7101 (8), *V* = 1857.77 (10)	6.65, 5.01, 1.34	1.48
2	$(BA)_2PbBr_2Cl_2$	*Pbca*	*a* = 8.1569 (2), *b* = 8.0286 (2), *c* = 27.7930 (5), *V* = 1820.14 (8)	8.14, 6.10, 1.70	2.04
3	$(BA)_2PbBrCl_3$	*Pbca*	*a* = 8.0636 (3), *b* = 7.9445 (2), *c* = 27.8237 (11), *V* = 1782.42 (13)	7.51, 5.64, 1.43	1.32
4	$(BA)_2PbCl_4$	*Pbca*	*a* = 7.9874 (15), *b* = 7.8600 (15), *c* = 27.975 (5), *V* = 1756.3 (6)	10.83, 7.93, 1.34	1.91
0	$(PMA)_2PbBr_4$	*Cmc*2$_1$	*a* = 33.4343 (7), *b* = 8.1494 (4), *c* = 8.1421 (4), *V* = 2218.45 (15)	7.42, 5.82, 1.70	2.05
1	$(PMA)_2PbBr_3Cl$	*Cmc*2$_1$	*a* = 33.5581 (11), *b* = 8.0505 (4), *c* = 8.0300 (4), *V* = 2169.4 (2)	7.60, 5.99, 1.70	2.22
2	$(PMA)_2PbBr_2Cl_2$	*Cmc*2$_1$	*a* = 33.5943 (12), *b* = 7.9695 (4), *c* = 7.9099 (4), *V* = 2117.72 (16)	9.36, 7.36, 2.02	2.76
3	$(PMA)_2PbBrCl_3$	*Cmc*2$_1$	*a* = 33.6422 (7), *b* = 7.8885 (4), *c* = 7.8186 (4), *V* = 2074.94 (16)	11.20, 8.64, 2.63	3.02
4	$(PMA)_2PbCl_4$	*Cmc*2$_1$	*a* = 33.6805 (6), *b* = 7.7416 (2), *c* = 7.8276 (2), *V* = 2040.98 (9)	11.25, 8.85, 2.39	3.84
0	$(PEA)_2PbBr_4$	*P*-1	*a* = 16.423(2), *b* = 17.5948(9), *c* = 25.977(3), *V* = 6758.5 (13)	14.07, 10.58, 4.20	7.04
1	$(PEA)_2PbBr_3Cl$	*P*-1	*a* = 16.264(2),	12.43, 9.04,	5.98

			b = 17.6092(8), *c* = 25.685(2), *V* = 6644.5 (11)	3.75	
2	$(PEA)_2PbBr_2Cl_2$	*P*-1	*a* = 16.107(2), *b* = 17.6392(9), *c* = 25.408(3), *V* = 6537.9 (13)	13.90, 10.48, 3.99	7.33
3	$(PEA)_2PbBrCl_3$	*P*-1	*a* = 15.9520(17), *b* = 17.6752(9), *c* = 25.193(3), *V* = 6438.5(11)	12.88, 9.94, 3.40	5.21
4	$(PEA)_2PbCl_4$	*P*-1	*a* = 15.8166(12), *b* = 17.7098(11), *c* = 24.969(3), *V* = 6342.3 (11)	13.60, 10.09, 3.63	7.87